Experimental aspects of QCD

1. Experimental observations motivating QCD
2. Recap: QCD Feynman-Rules and color factors
3. Discovery of the gluon and its spin
4. $q\bar{q} \rightarrow q\bar{q}$: s- and t-channel process
5. Measurement of alphas and its running

1. Experimental observations motivating QCD

Recap:

Hadron matter made of quarks of different flavor (static quark model):
Approximate SU(3) flavor symmetry for light quarks: u ↔ d ↔ s

$$Y^f = \frac{1}{\sqrt{3}}\lambda_8$$

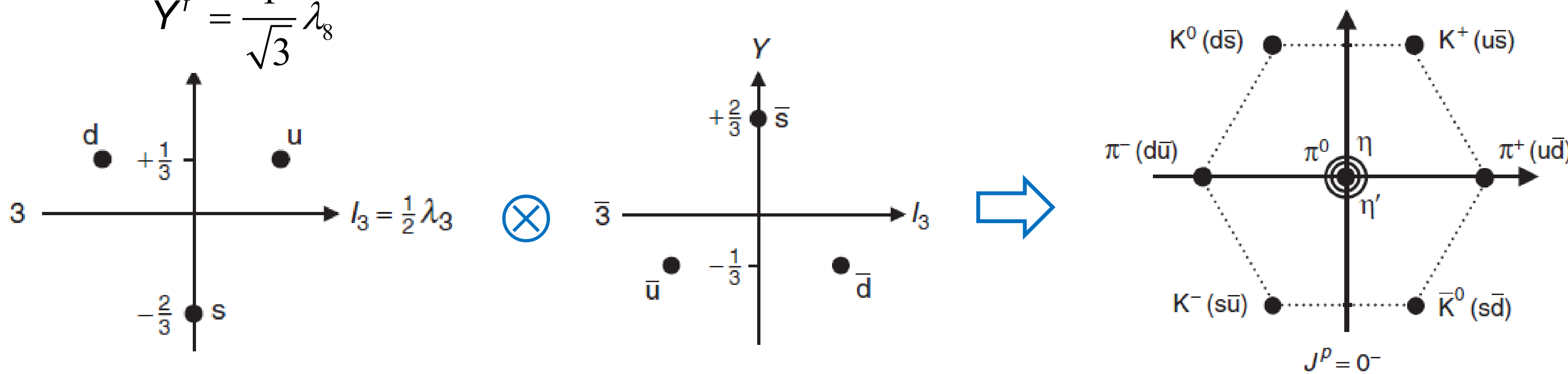

DIS experiments provided existence proof of point-like spin ½ constituents of the proton.

Color quantum number

Historically, an additional internal quantum number “color charge” with 3 possible values (often called r, g, b, or correspondingly $\bar{r}$, $\bar{g}$, $\bar{b}$ for anti-quarks) was introduced to cure a symmetry-problem of the Δ^{++} (u↑ u↑u↑ , J=3/2) quark wave function:

$$\Psi(uuu,\uparrow\uparrow\uparrow) = \underbrace{\psi_{space} \cdot \phi_{flavor} \cdot \chi_{spin}}_{\text{symmetric under particle exchange}} \cdot \xi_{color}$$

with $\psi_{space} =$ symmetric (L=0)

$\phi_{flavor} =$ symmetric (uuu)

$\chi_{spin} =$ symmetric (↑↑↑)

⇨ Need additional color wave function ξ_{color} fully anti-symmetric

$$\xi_{color} = \frac{1}{\sqrt{6}} \sum_{i,j,k} \varepsilon_{ijk} u_i u_j u_k$$ with color indices i, j, k

Experimental evidence for 3 different "color states": $N_C = 3$

Hadronic cross section $e^+e^- \rightarrow q\bar{q}$

$$R_{had} = \frac{\sigma_{had}}{\sigma_{\mu\mu}} = N_C \cdot \sum_f Q_f^2$$

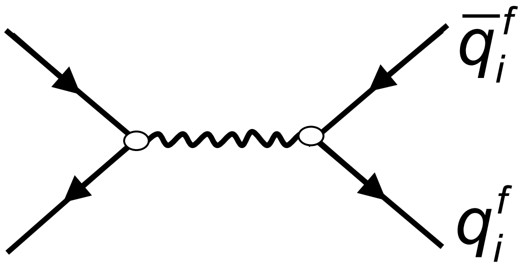

f flavor

i color

(we discussed R_{had} already)

Since the color of a quark cannot be observed
we postulate a SU(3) color symmetry: r ↔ g ↔ b

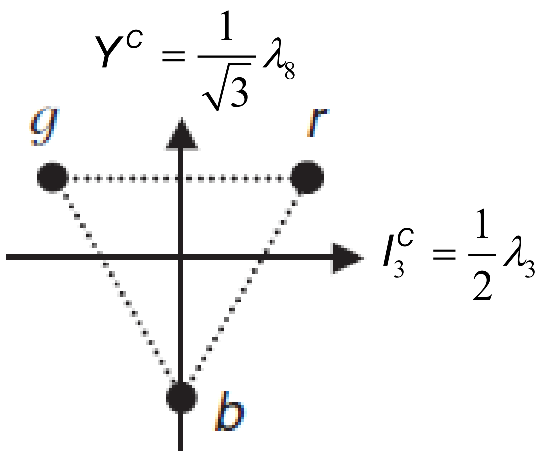

<u>Reminder:</u>

In the fundamental representation the generator T_a of SU(3) are given by the 8 Gell-Mann matrices λ_a with a=1…8: $T_a = ½\ \lambda_a$ (see QCD).

The 3x3 Gell-Mann matrices λ_a are traceless, hermitian and unitary.

Reminder Gell-Mann matrices (Recap)

SU(3) Generators: $T_a = \frac{1}{2}\lambda_a$

Gell-Mann matrices:

$$\lambda_1 = \begin{pmatrix} 0 & 1 & 0 \\ 1 & 0 & 0 \\ 0 & 0 & 0 \end{pmatrix}, \quad \lambda_2 = \begin{pmatrix} 0 & -i & 0 \\ i & 0 & 0 \\ 0 & 0 & 0 \end{pmatrix}, \quad \lambda_3 = \begin{pmatrix} 1 & 0 & 0 \\ 0 & -1 & 0 \\ 0 & 0 & 0 \end{pmatrix}$$

$$\lambda_4 = \begin{pmatrix} 0 & 0 & 1 \\ 0 & 0 & 0 \\ 1 & 0 & 0 \end{pmatrix}, \quad \lambda_5 = \begin{pmatrix} 0 & 0 & -i \\ 0 & 0 & 0 \\ i & 0 & 0 \end{pmatrix}, \quad \lambda_6 = \begin{pmatrix} 0 & 0 & 0 \\ 0 & 0 & 1 \\ 0 & 1 & 0 \end{pmatrix},$$

$$\lambda_7 = \begin{pmatrix} 0 & 0 & 0 \\ 0 & 0 & -i \\ 0 & i & 0 \end{pmatrix}, \quad \lambda_8 = \frac{1}{\sqrt{3}} \begin{pmatrix} 1 & 0 & 0 \\ 0 & 1 & 0 \\ 0 & 0 & -2 \end{pmatrix}$$

Lie-Algebra:

$$[T_a, T_b] = i f_{abc} T_c$$

f_{abc} anti-symmetric SU(3) structure constants w/ $f_{acd} f_{bcd} = N_C \delta_{ab}$

$$tr(T_a T_b) = \frac{1}{2}\delta_{ab}$$

2. QCD Feynman rules and color factors (recap)

Requiring local gauge invariance introduces 8 vector fields A_a^μ (gluon fields) and the quark-gluon interaction which depends on the color index i of the quarks:

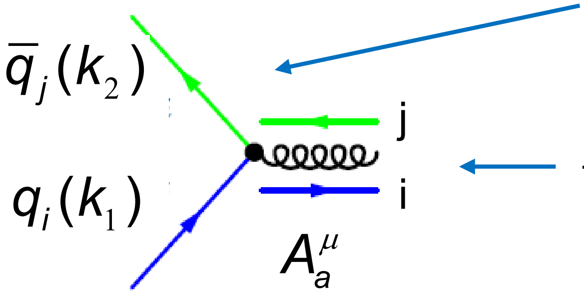

Color flow

$$-ig_s(T_a)_{ji}\bar{q}_j(k_2)\gamma^\mu q_i(k_2)$$ (coupling quark current)

Gluon propagator

$$-\frac{g_{\mu\nu}}{q^2+i\varepsilon}\delta_{ab}$$

As pointed out by Tilman, the color specific factors and the and Dirac algebra of the γ matrices factorize → relevant traces of Gell-Man matrices separate.

$$|M|^2 \sim (T_a)_{ji}(T_b)_{ij} = tr(T_a T_b)$$

Due to the non-abelian structure there are in addition triple and quartic gluon couplings:

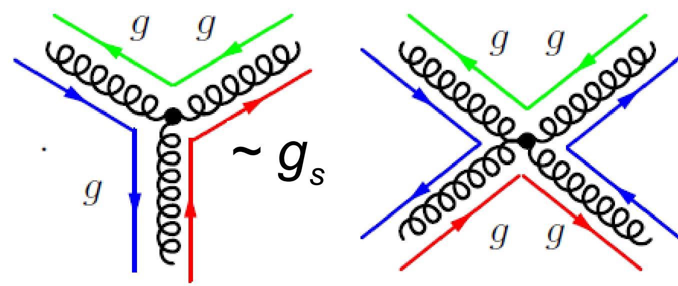

$\sim g_s$ $\sim g_s^2$

QCD color flow for "pedestrians" I

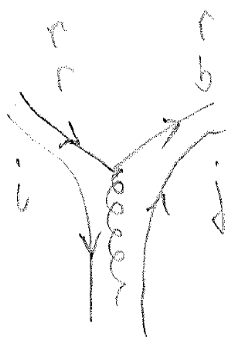

gluon carries color and anti-color, represented by $(T_a)_{ji}$ to couple corresponding color states q_i and $\bar{q}_j$

Chosing the representation

$$|r\rangle = \begin{pmatrix}1\\0\\0\end{pmatrix} \quad |g\rangle = \begin{pmatrix}0\\1\\0\end{pmatrix} \quad |b\rangle = \begin{pmatrix}0\\0\\1\end{pmatrix}$$

one has combinations such as

$$\langle r|T_a|r\rangle = \frac{1}{2}(\lambda_a)_{11}$$

$$\langle b|T_a|r\rangle = \frac{1}{2}(\lambda_a)_{31}$$

3. Discovery of the gluon & determination of gluon spin

$$e^+e^- \rightarrow q\bar{q}$$

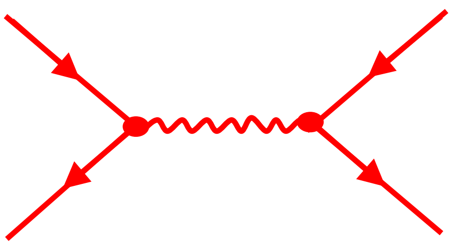

local parton
hadron duality

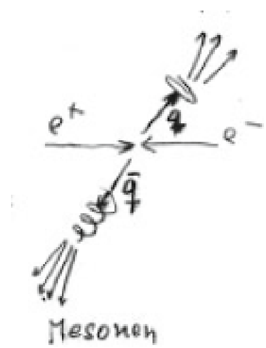

One of the first 2-jet events at PETRA

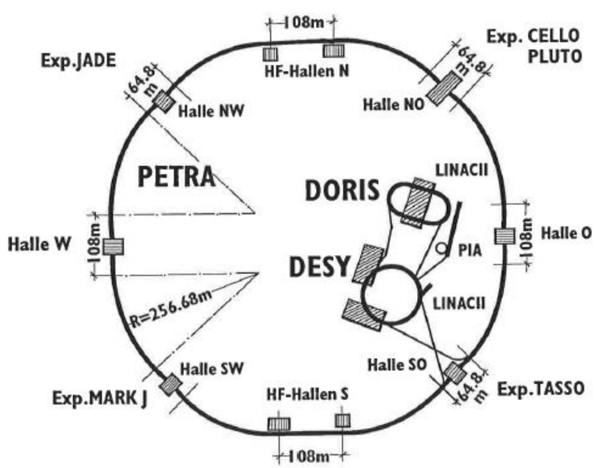

Remark:

PETRA (1978 -) was e^+e^- circular accelerator at DESY: operated at $\sqrt{s}$ between 13 and 46 GeV.

Earlier e^+e^- machines (e.g. SPEAR) with $\sqrt{s}_{max} \approx$ 10 GeV: $ee \rightarrow qq$ events have been observed, however events much less jet-like (more spherical) due to the smaller boost.

Quantify the 2-jet-likeness: thrust T

$$T = \max \frac{\sum_i |\vec{p}_i \cdot \vec{n}_T|}{\sum_i |\vec{p}_i|}$$

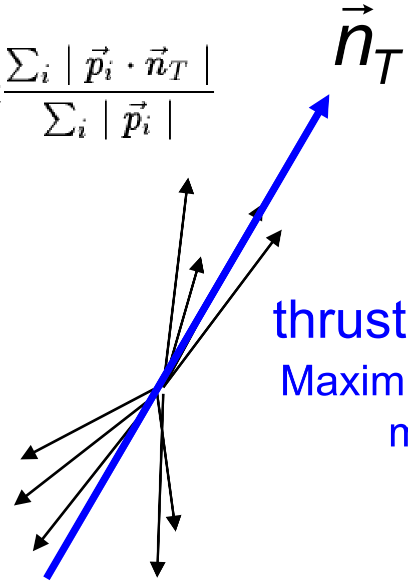

thrust axis = jet axis

Maximizes longitudinal momentum

Expect T close to 1 ⇨

Thrust distribution

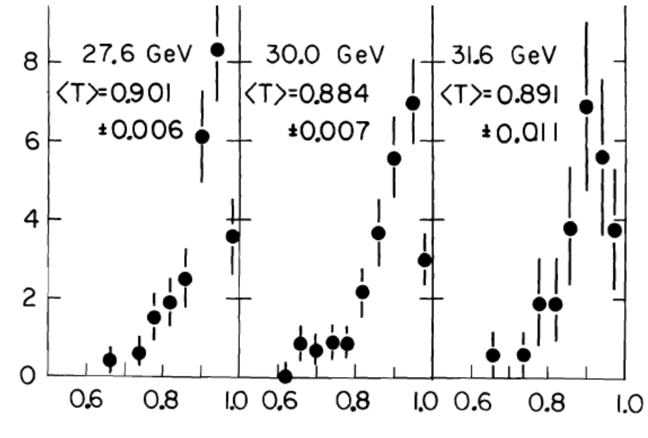

Thrust axis also defines the jet-axis

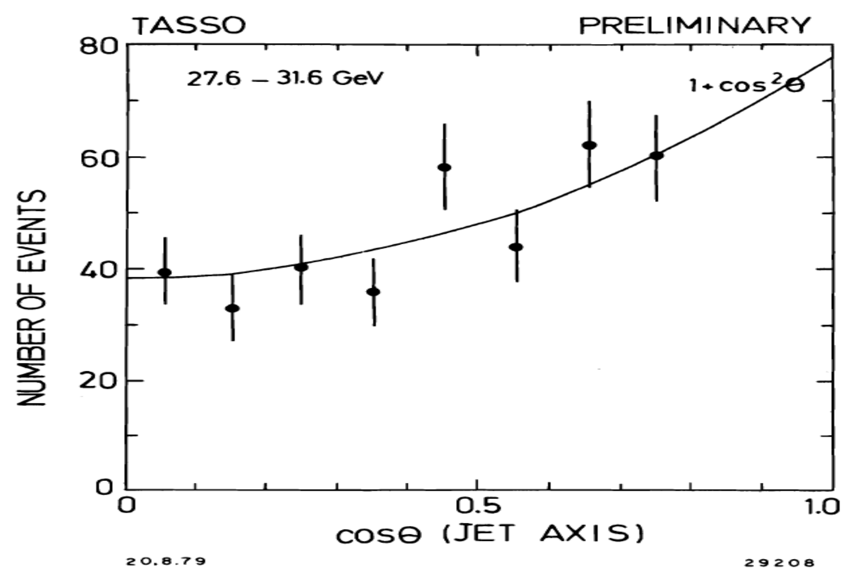

Jet axis follows $(1+\cos^2\theta)$

⇨ Quark spin ½

3-jet events:

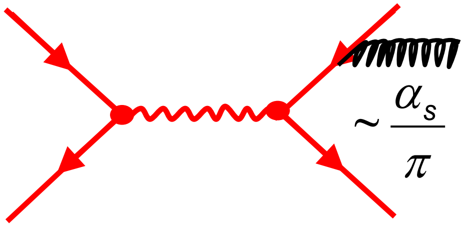

$\sim \frac{\alpha_s}{\pi}$

planar

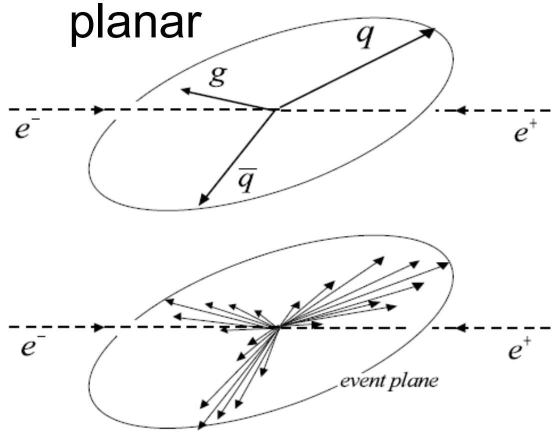

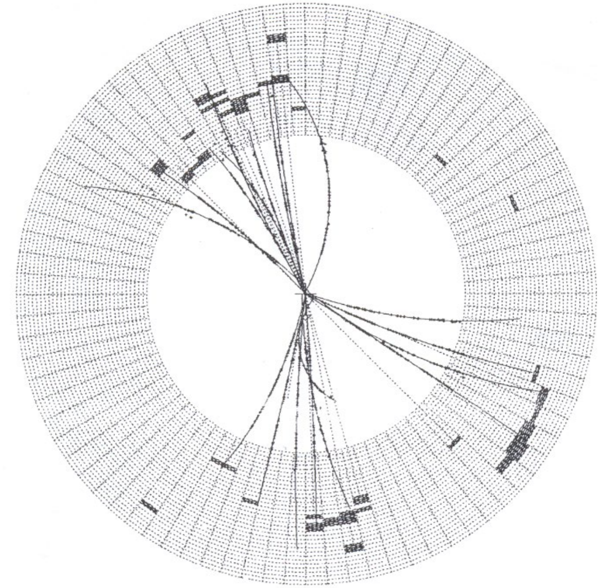

Fig. 11.12 A three-jet event observed by the JADE detector at PETRA.

But: How to exclude that the observed 3-jet signatures are fluctuations?

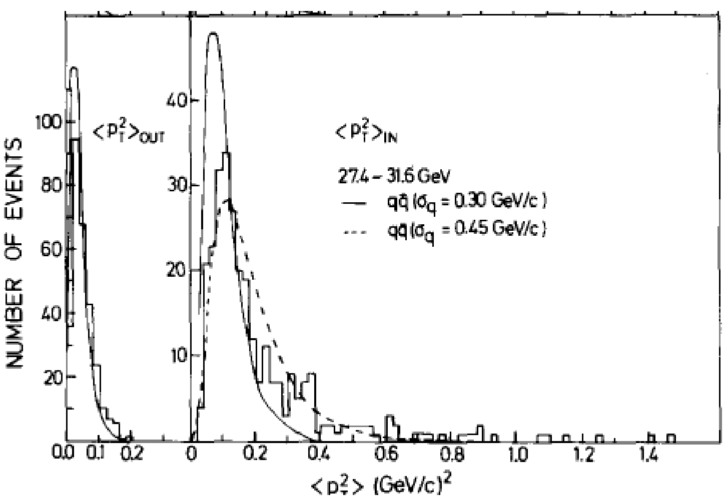

Check transverse $<p_T^2>$ outside and inside event plane: fluctuations should be the same: Outside $<p_T^2>$ well described by 2-jet model. Inside: "broadening" cannot be described, even not by higher string-tension.

Exp: $$\frac{\#3-\text{jet events}}{\#2-\text{jet events}} \approx 0.15 \sim \frac{\alpha_s}{\pi}$$

Spin of the Gluon:

Angular distribution of jets depend on gluon spin:

Ordering of 3 jets: $E_1 > E_2 > E_3$

Likely to be gluon

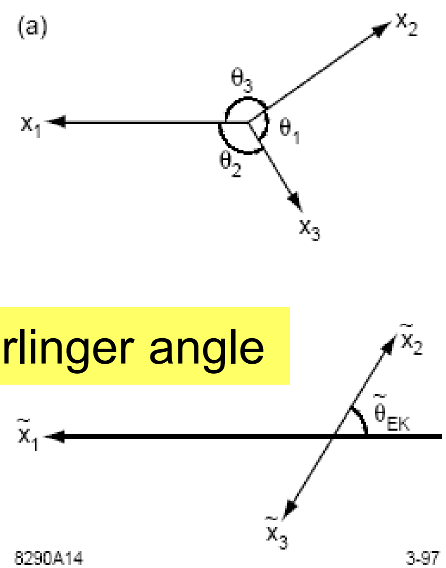

Ellis-Karlinger angle

Figure 8: (a) Representation of the momentum vectors in a three-jet event, an (b) definition of the Ellis-Karliner angle.

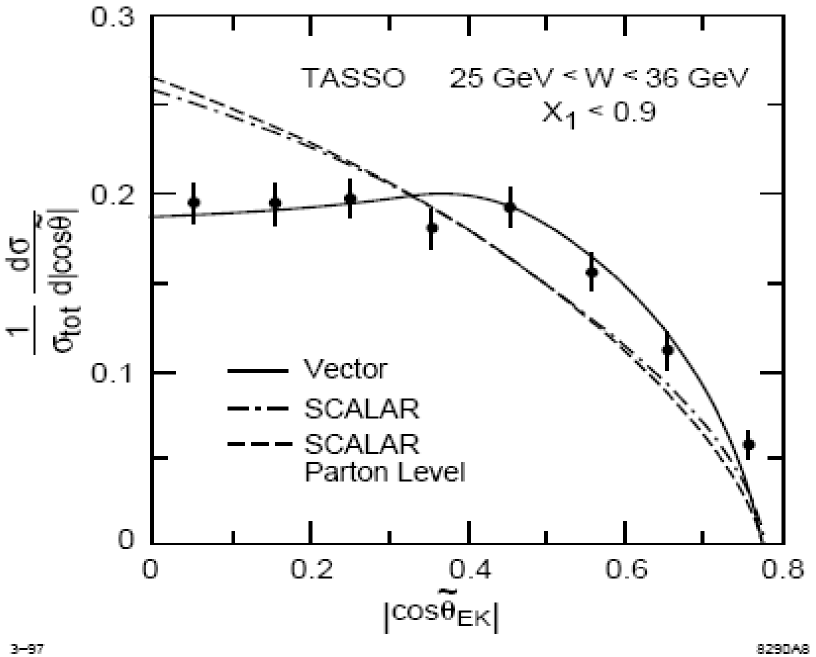

Figure 9: The Ellis-Karliner angle distribution of three-jet events recorded by TASSO at $Q \sim 30$ GeV [18]; the data favour spin-1 (vector) gluons.

Measure direction of jet-1 in the rest frame of jet-2 and jet-3: θ_{EK}

Gluon spin J=1

4. $q\bar{q} \rightarrow q\bar{q}$: s- and t-channel process

The easiest process to calculate is, e.g. $q\bar{q} \rightarrow b\bar{b}$ at tree-level.

Processes w/ external gluons require to think about the ghost-fields (ξ =1 gauge).

$$q\bar{q} \rightarrow b\bar{b}$$

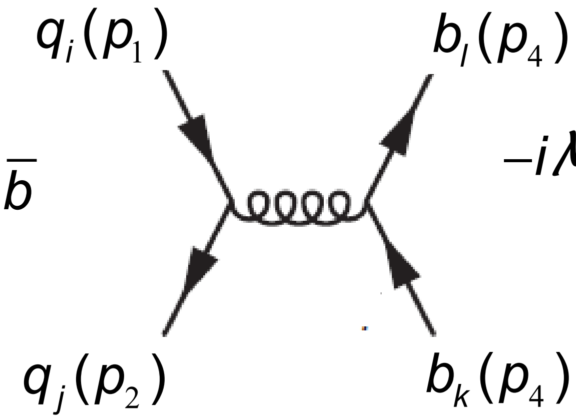

$$-i\mathcal{M} = -ig_s(T_a)_{ji}\bar{q}_j(p_2)\gamma^{\mu}q_i(p_1)\left(-\frac{g_{\mu\nu}}{q^2}\delta_{ab}\right)$$

$$-ig_s(T_b)_{lk}\bar{b}_l(p_3)\gamma^{\nu}b_k(p_4)$$

$$= g_s^2 \cdot \underbrace{(T_a)_{ji}(T_a)_{lk}} \cdot (\ldots QED\ldots)$$

$$= g_s^2 \cdot C(i\,\bar{j} \rightarrow l\,\bar{k}) \cdot (\ldots QED\ldots)$$

To calculate $\langle |\mathcal{M}|^2 \rangle$ we need $\langle |C|^2 \rangle$

$$\langle |C|^2 \rangle = \frac{1}{9} \sum_a \sum_{i,j,k,l} |C(i\,j \to k\,l)|^2$$

$$= \frac{1}{9} \sum_{a,b} \left| \left(tr(T_a T_b) \right) \right|^2 = \frac{1}{9} \sum_{a,b} \left| \left(\frac{1}{2} \delta_{ab} \right) \right|^2 = \frac{1}{9} \frac{8}{4} = \frac{2}{9}$$

See QCD lecture

w/ QED matrix element:

replace e $\leftrightarrow$ g_s

$$\langle |\mathcal{M}|^2 \rangle = 2e^2 \left(\frac{t^2 + u^2}{s^2} \right)$$

$$\langle |\mathcal{M}(q\bar{q} \to b\bar{b})|^2 \rangle = 2g_s^2 \langle |C|^2 \rangle \left(\frac{t^2 + u^2}{s^2} \right) = 2g_s^2 \frac{2}{9} \left(\frac{t^2 + u^2}{s^2} \right)$$

Color factors for "pedestrians" II

Color factors for $q\bar{q} \to b\bar{b}$:

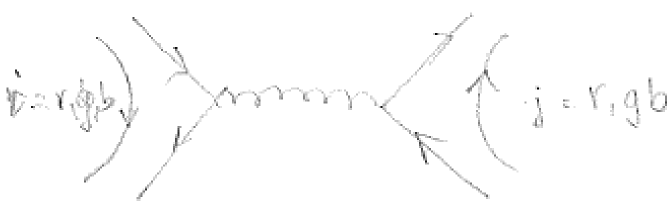

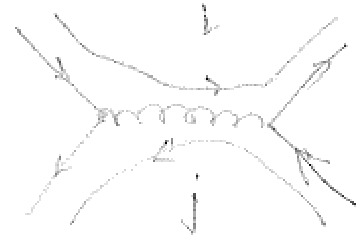

e.g.: $r\bar{r} \to r\bar{r}$

$$C(r\bar{r} \to r\bar{r}) = \frac{1}{4} \sum_a (\lambda_a)_{11} (\lambda_a)_{11}$$

$$= \frac{1}{4}\left[(\lambda_3)^2_{11} + (\lambda_8)^2_{11} \right]$$

$$= \frac{1}{4}\left[1^2 + \left(\frac{1}{\sqrt{3}}\right)^2 \right] = \frac{1}{3}$$

$$C(r\bar{b} \to r\bar{b}) = \frac{1}{4} \sum_a (\lambda_a)_{13} (\lambda_a)_{31} = \frac{1}{4}\left[(\lambda_4)_{13} (\lambda_4)_{31} + (\lambda_5)_{13} (\lambda_5)_{31} \right] = \frac{1}{2}$$

t - channel

$$(T_a)_{ji}\,(T_a)_{lk}$$

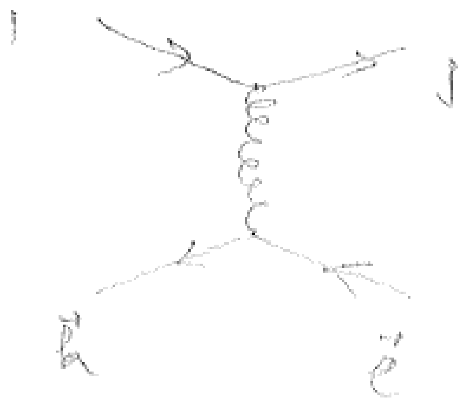

$$(T_a)_{ji}\,(T_a)_{kl}$$

$q\bar{q}$ QCD potential ("t-channel"):

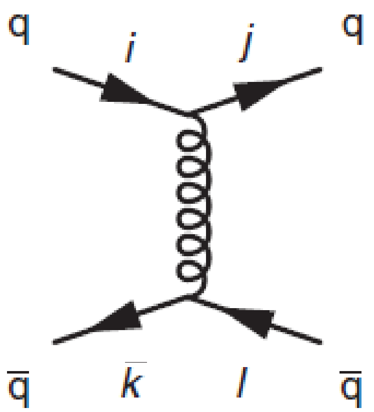

In QED: attractive potential.

$$V(\vec{q}) = -\frac{e^2}{|\vec{q}|^2} \quad \text{(in momentum space)}$$

$$\Downarrow$$

In QCD:

$$V(\vec{q}) = -(T_a)_{ij}(T_a)_{lk} \cdot \frac{g_s^2}{|\vec{q}|^2}$$

For the quark-antiquark pair there are two different configurations possible:

- Color singlet: $|q\bar{q}\rangle_S = \delta_{ik} |q_i \bar{q}_k\rangle$

  $$C = \delta_{ik} C(i\,\bar{k} \to j\,\bar{l}) = C_F \delta_{jl} = \frac{4}{3}$$

- Color octet: $|q\bar{q}\rangle_8 \sim (T_a)_{ki} |q_i \bar{q}_k\rangle$

  $$C = (T_a)_{ki} C(i\,\bar{k} \to j\,\bar{l}) \sim (T_a T_b T_a)_{jl} = -\frac{1}{2N_C}(T_a)_{jl}$$

Summary $q\bar{q}$-potential

$$V(\vec{q}) = -\frac{g_s^2}{|\vec{q}|^2} \cdot C \quad \text{with} \quad C = \begin{cases} C_F & \text{for color singlet: attractive} \\ -\dfrac{1}{2N_C} & \text{for color octet: repulsive} \end{cases}$$

This is consistent w/ the fact that only color singlet $q\bar{q}$ pairs are observed as bound states (mesons) in nature.

5. Running of strong coupling constant α_s

Recap: $$\frac{1}{\alpha_s(M^2)} = \frac{1}{\alpha_s(p^2)} - b_0 \log\frac{p^2}{M^2} + \mathcal{O}(\alpha_s)$$ (QCD lecture)

Strong coupling $\alpha_s(q^2)$

$$\alpha_s(q^2) = \frac{\alpha_s(\mu^2)}{1 + \alpha_s(\mu^2) b_0 \log\frac{q^2}{\mu^2}}$$

μ^2 = renormalization scale

$$b_0 = \frac{1}{4\pi}\left(\frac{11}{3}N_c - \frac{2}{3}n_f\right)$$

n_f = active quark flavors

← In QED similar function but w/o first term ~N_C → different sign!!

$$\alpha_s(q^2) = \frac{1}{b_0 \log(q^2/\Lambda^2_{QCD})}$$

with $\Lambda_{QCD} \approx 210\,\text{MeV}$

scale at which perturbation theory diverges

Measurement of q^2 dependence of α_s

➡ α_s measurements are done at given scale q^2: $\alpha_s(q^2)$

a) α_s from total hadronic cross section in QED or at Z pole

$e^+e^- \to q\bar{q}(g)$

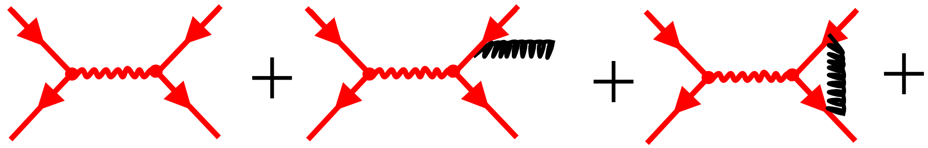

+ higher orders

$$\sigma_{had}(s) = \sigma_{had}^{QED}(s)\underbrace{\left[1 + \frac{\alpha_s(s)}{\pi} + 1.4 \cdot \frac{\alpha_s(s)^2}{\pi^2} + \ldots\right]}_{1+\delta_{QCD}}$$

$$R_{had} = \frac{\sigma(ee \to hadrons)}{\sigma(ee \to \mu\mu)} = 3\sum Q_q^2 \left[1 + \frac{\alpha_s(s)}{\pi} + 1.4 \cdot \frac{\alpha_s(s)^2}{\pi^2} + \ldots\right] \qquad \text{(QED)}$$

Recap

Measurement of $e^+e^- \to$hadrons and R_{had}

$$R_{had} = \frac{\sigma(e^+e^- \to \text{hadrons})}{\sigma(e^+e^- \to \mu^+\mu^-)} = \frac{\sigma_{had}}{\sigma_{\mu\mu}}$$

$$R_{had} = N_C \cdot \sum_{quarks\ i} Q_i^2 =$$

$\sqrt{s}$	Quarks	$R_{had} = 3 \cdot \sum_i Q_i^2$
< ~3 GeV	uds	3·6/9=2.00
< ~10 GeV	udsc	3·10/9=3.33
< ~350 GeV	udscb	3·11/9=3.67

Data lies systematically higher than the prediction from Quark Parton Model (QPM) → QCD corrections

$$\sigma(s) = \sigma_{QED}(s)\left[1 + \frac{\alpha_s(s)}{\pi} + 1.4 \cdot \frac{\alpha_s(s)^2}{\pi^2} + \dots\right]$$

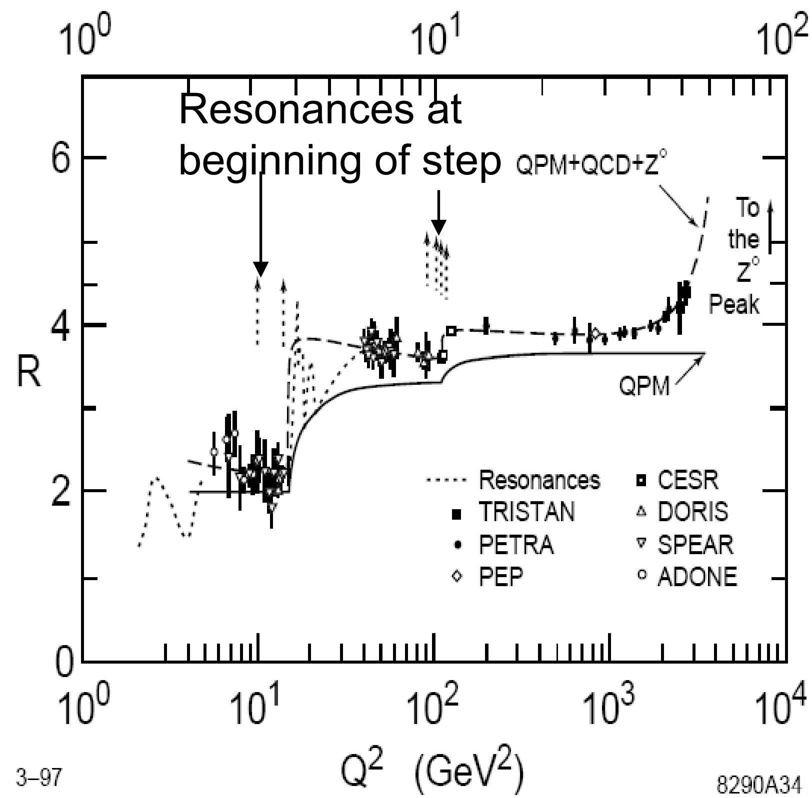

Z pole:

At the Z-pole instead of the electric charge the relevant couplings are c_L and c_R of the quarks and the muon to the Z.

However QCD corrections stay the same:

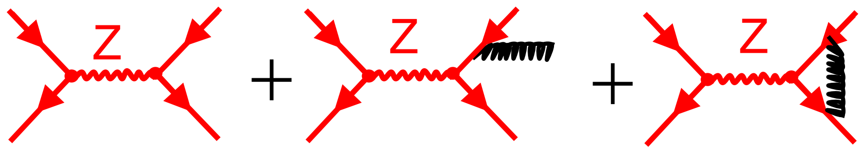

+ higher orders

$$\sigma_{had}(s) = \sigma^Z_{had}(s)\underbrace{\left[1 + \frac{\alpha_s(s)}{\pi} + 1.4 \cdot \frac{\alpha_s(s)^2}{\pi^2} + \ldots\right]}_{1+\delta_{QCD}}$$

for $\sigma^Z_{had}(s)$ look at EW lecture

$$\sigma(s) = 12\pi \frac{\Gamma_e \Gamma_\mu}{M_Z^2} \cdot \frac{s}{(s - M_Z^2)^2 + M_Z^2 \Gamma_Z^2}$$

$$\Gamma_f = \frac{\alpha M_Z}{12 \sin^2\theta_w \cos^2\theta_w} \cdot \left[(g_V^f)^2 + (g_A^f)^2\right]$$

Early Z-pole measurement:

$$R^Z_{had} = 20.89 \pm 0.13$$

$$\delta_{QCD} = 0.0461 \pm 0.0065$$

$$\alpha_s(m_z) = 0.136 \pm 0.019$$

b) α_s from hadronic event shape variables

3-jet rate: $R_3 \equiv \frac{\sigma_{3-jet}}{\sigma_{had}}$ depends on α_s

3-jet rate is measured as function of Jet resolution

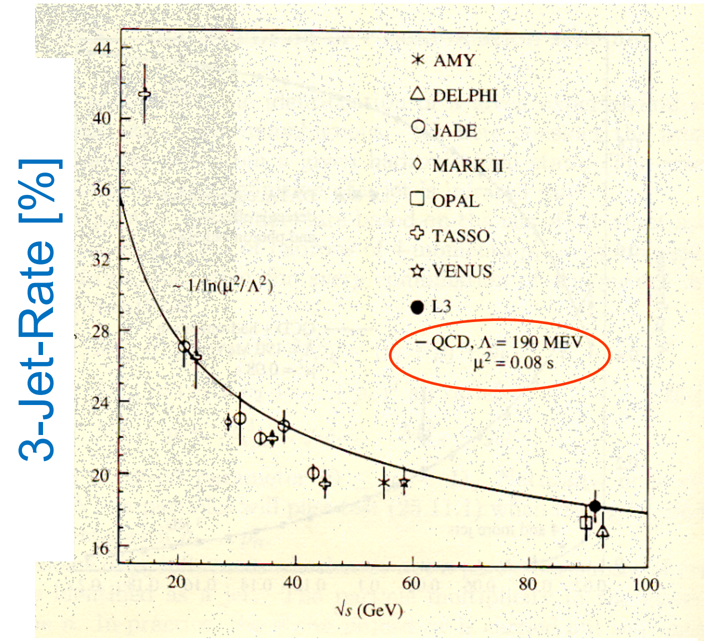

QCD calculation provides a theoretical prediction for $R_3^{theo}(\alpha_s)$

→ fit $R_3^{theo}(\alpha_s)$ to the data to determine α_s

Other event shape variables (sphericity, thrust,…) can be used to obtain a prediction for α_s

$$T = \max \frac{\sum_i |\vec{p}_i \cdot \vec{n}_T|}{\sum_i |\vec{p}_i|}$$

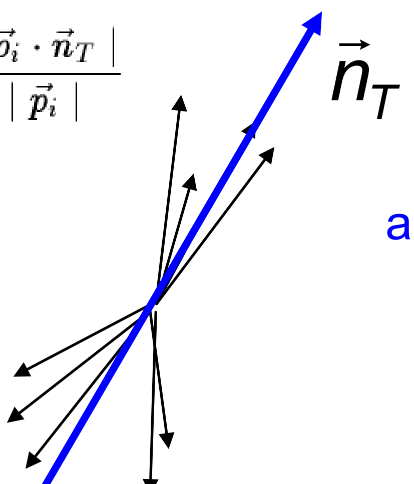

also function of α_s

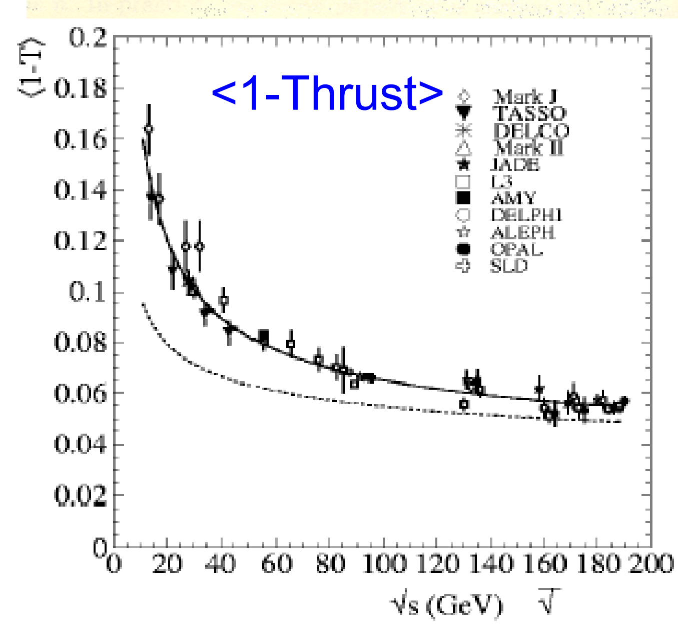

Jet Algorithms (next semester)

Iterative Jet algorithms ("Jade"-type, developed for $e^+ e^-$)

1) for all pairs of particles i, j calculate distance parameter y_{ij}

2) find pair i, j with smallest $y_{ij,\,\min}$

3) add 4-momenta: $p_i + p_j = p_k$ replace p_i, p_j by p_k

4) iterate till $y_{ij} > y_{cut}$

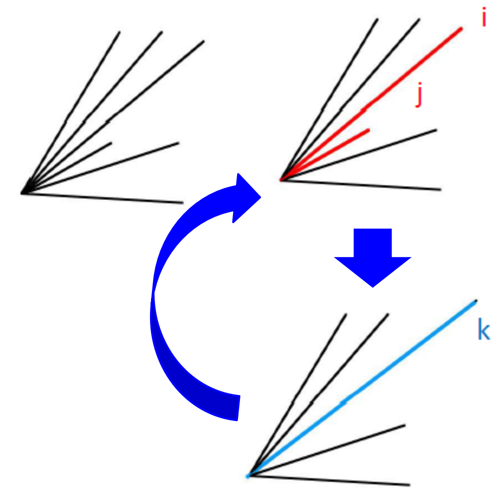

Distance measures:

$$y_{ij} = 2\,\frac{E_i\,E_j\,(1-\cos\theta_{ij})}{s}$$

Jade algorithm: IRCS but theoretically difficult; large higher order correction.
(invariant mass squared)

$$y_{ij} = 2\,\frac{\min(E_i^{\,2}, E_j^{\,2})(1-\cos\theta_{ij})}{s}$$

k_T – algorithm:
better higher order behavior
(relative transverse momentum squared)

$$\min(E_i^2, E_j^2) \rightarrow \min(E_i^{-2}, E_j^{-2})$$

anti-k_T – algorithm: often used nowadays
(→jets with only soft radiation are conical)

c) α_s from hadronic τ decays

$$R^{\tau}_{had} = \frac{\Gamma(\tau \rightarrow \nu_{\tau} + Hadrons)}{\Gamma(\tau \rightarrow \nu_{\tau} + e\overline{\upsilon}_{e})} \sim f(\alpha_s)$$

$$R^{\tau}_{had} =$$

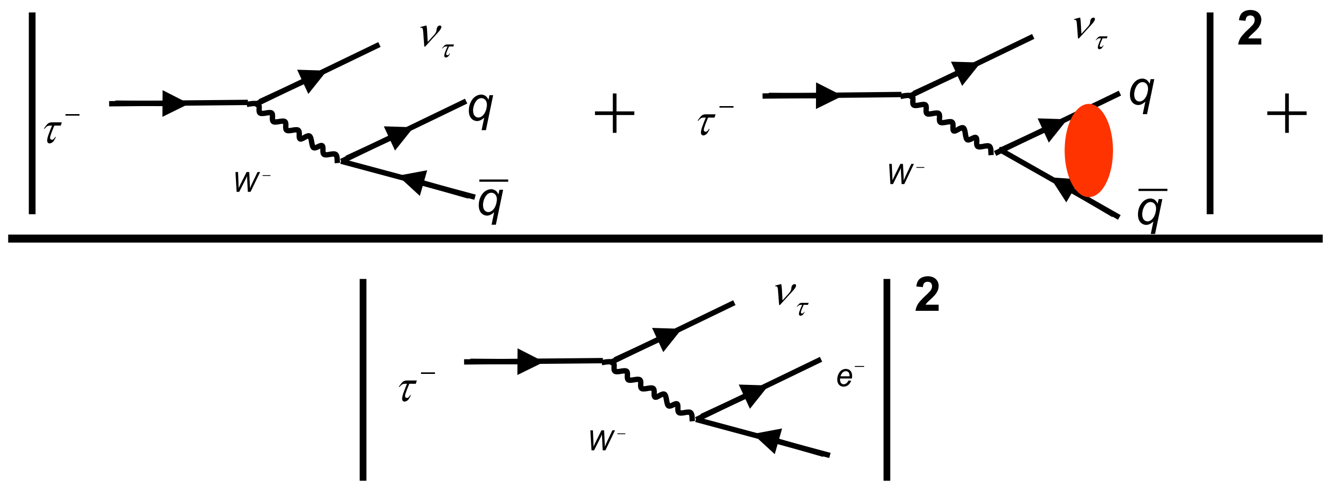

$$R^{\tau}_{had} = R^{\tau,0}_{had}\left(1 + \frac{\alpha_s(m_\tau^2)}{\pi} + \ldots\right)$$

d) α_s from DIS (deep inelastic scattering): DGLAP fits to PDFs (next semester)

Running of α_s and asymptotic freedom

Experimental determination.

$$\alpha_s(M_Z^2) = 0.1175 \pm 0.0010$$

Alphas from the lattice:

$$\alpha_s(M_Z^2) = 0.1182 \pm 0.0008$$

Unweighted average w/ average uncertainty of the two:

$$\alpha_s(M_Z^2) = 0.1179 \pm 0.0009$$

Particle Data Group 2021

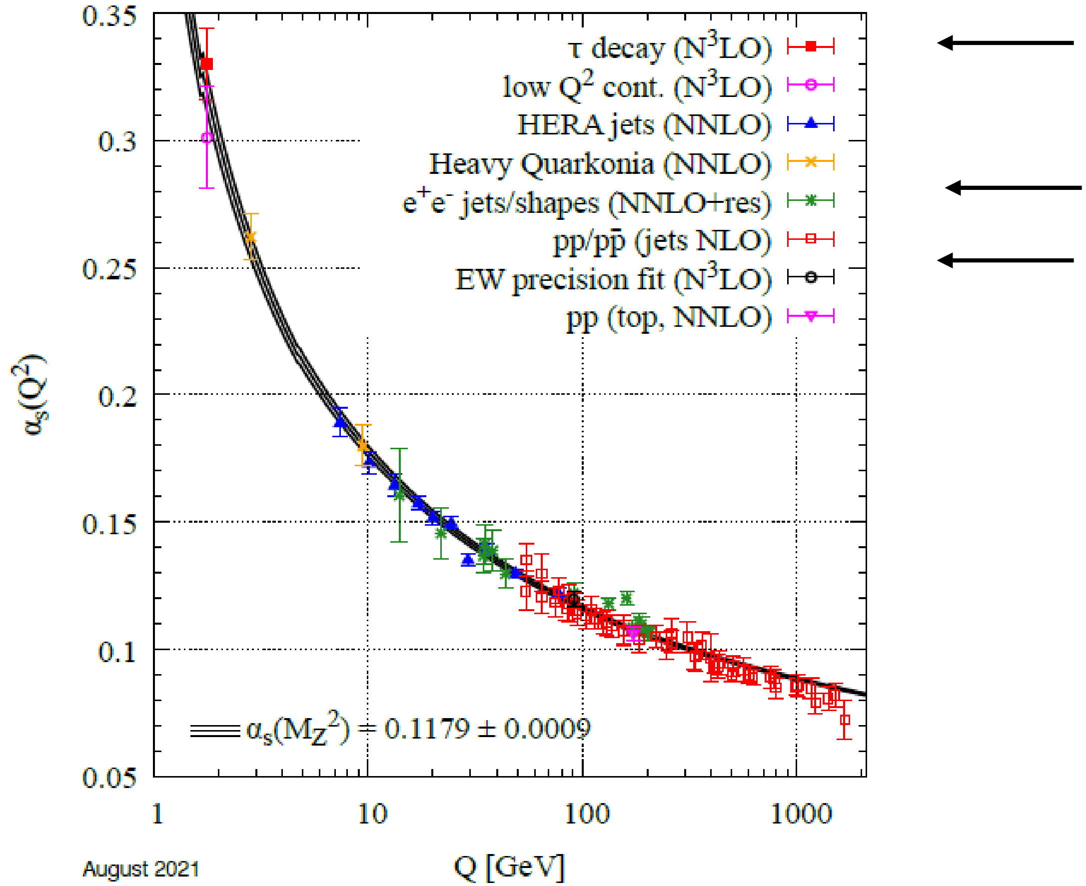

Figure 9.3: Summary of measurements of α_s as a function of the energy scale Q. The respective degree of QCD perturbation theory used in the extraction of α_s is indicated in brackets (NLO: next-to-leading order; NNLO: next-to-next-to-leading order; NNLO+res.: NNLO matched to a resummed calculation; N^{3}LO: next-to-NNLO).